RADAR SCATTERING FROM SNOW FACIES OF THE GREENLAND ICE SHEET: RESULTS FROM THE AIRSAR 1991 CAMPAIGN

E. Rignot, K. Jezek*, J.J. van Zyl, M.R. Drinkwater, and Y.L. Lou.

Jet Propulsion Laboratory, California Institute of Technology, Pasadena CA 91109
*Ohio State University, Byrd Polar Research Center, Columbus, OH 43210

ABSTRACT

In June 1991, the NASA/Jet Propulsion Laboratory airborne SAR (AIRSAR) collected the first calibrated multi-channel SAR observations of the Greenland ice sheet. Large changes in radar scattering are detected across different melting zones. In the dry-snow zone, Rayleigh scattering from small snow grains dominates at C-band. In the soaked-snow zone, surface scattering dominates, and an inversion technique was developed to estimate the dielectric constant of the snow. The radar properties of the percolation zone are in contrast unique among terrestrial surfaces, but resemble those from the icy Galilean satellites. The scatterers responsible for the percolation zone unusual echoes are the massive ice bodies generated by summer melt in the cold, dry, porous firn. An inversion model is developed for estimating the volume of melt-water ice retained each summer in the percolation zone from multi-channel SAR data. The results could improve current estimates of the mass balance of Greenland, and could help monitor spatial and temporal changes in the strength of summer melt in Greenland with a sensitivity greater than that provided by altimeters.

INTRODUCTION

An understanding of the geophysical characteristics of polar ice sheets and snow masses and of their time evolution with changing environmental conditions is essential to climate modeling. The first examples of SAR observations of the Greenland ice sheet [1-4] have shown great promise for monitoring applications of the changing hydrology of polar ice sheets as a result of atmospheric warming. Here, we report result from the first calibrated multi-channel SAR observations of Greenland collected by AIRSAR in June 1991. The goals of the experiment were to record radar echoes from different melting zones of the Greenland ice sheet and then to relate these radar observations to the snow and firn physical properties. Fig. 1 shows the flight track of AIRSAR; the location of 3 ice camps where glaciologists recorded snow stratigraphy, grain size, density, and temperature; and the 4 melting zones characterizing different degrees of melting of the ice sheet in the summer [5].

AIRSAR operates at C-, L-, and P- band frequencies (5.6, 24, and 68-cm wavelengths), and records the complete scattering matrix of each resolution element at each frequency. The radar echoes are internally calibrated. The calibration was cross-checked using the radar responses of trihedral corner reflectors deployed at Crawford Point prior to flight. The results indicate a calibration accuracy better than 1-2 dB for $\theta \geq 30°$. For $\theta \leq 30°$, the C-band radar cross-sections are underestimated by a few dBs, whereas the polarimetric characteristics seem correct. Radiometric calibration errors may be caused by processing artifacts due to the shorter integration time, or to errors in the predicted response from corner reflectors which point more than 15° away from the radar lobe direction. The system noise level, dominated by thermal noise from the radar receiver, varies with the receiver's gain settings, frequency, polarization, and also with the range distance after range and azimuth compressions. The SNR was found to be large over the percolation facies, but poor in the soaked- and dry-snow facies at large incidence angles. The apparent increase in σ^o_{HV} for $\theta \geq 60°$ in Fig. 2 is due to thermal noise and not to scattering.

ANALYSIS OF RADAR SCATTERING

We examined SAR scenes collected in 3 of the 4 melting snow zones of Fig. 1. The most striking observations are from the percolation zones, but interesting results are also obtained in the dry- and soaked-snow zones.

Dry-snow zone: Radar returns are low at all 3 frequencies, and mostly diffuse at C-band, which is consistent with volume scattering from dry snow grains. Model predictions based on Rayleigh scattering from a half-space of dry-snow agree with the AIRSAR measurements at C-band (Fig. 2), but underestimates the radar returns at L- and P-band. The longer wavelengths are probably sensitive to more deeply buried denser snow layers of larger snow grains, with a reduced pore space. Additional scenes will be processed to detect eventual spatial variations in snow properties within the dry snow zone.

Soaked-snow zone: Video imagery and 35 mm photos taken during the AIRSAR flight show that areas of low backscatter in the C-band imagery (Fig. 3) have also low radiances at visible optical frequencies and likely correspond to areas of wet snow accumulating in local surface depressions and surrounded by drier snow patches. C-band radar returns are low in wet snow because the snow layer is smooth and highly reflective, and are high in dry snow because of volume scattering from snow grains. Spatial variations in radar backscatter at L-band (not shown) are different, a result of the deeper penetration of the radar signals, revealing subsurface features of higher radar reflectivity among the wet snow patches detected at C-band. P-band data (not shown) reveal buried cracks and crevasses that are not visible at C-band.

We used the inversion technique of van Zyl et al. [7] to infer the dielectric constant ϵ_r and the rms height h of the reflecting surface from the SAR scene of Fig. 3. The algorithm is valid for natural terrain dominated by surface scattering, and uses HH- and VV- polarization at one frequency, preferably one for which $\lambda >> h$. The results at C-band are not satisfactory in dry snow areas because volume scattering from snow grains is falsely interpreted as resulting from rough surface scattering. The corresponding pixels can be separated using $\sigma^o_{HV} >$ - 28 dB. Pixels for which $h \geq 5$ cm, which corresponds to snow-free bedrock, are also removed because the estimation of ϵ_r is not reliable. In the remaining areas, ϵ_r and h have consistent values across range (the inversion technique is robust with incidence angle variations): h = 0.8 ±0.3 cm, a smooth surface, and ϵ_r = 3.0 ±0.5, i.e. wet snow with a liquid water content about 10±2% (Fig. E.33 [8]), which is within the range of values measured at the Swiss Camp. In addition, the inversion results reveal patches of standing water or thawed lakes ($\epsilon_r \geq 20$), as verified from the video imagery. These water formations would be difficult to identify from C-band VV or L-band HH data alone, illustrating the interest of polarimetric information. At L-band, the results are complicated by the deeper penetration of the signal. ϵ_r of "wet snow areas" is ≈ 3, but $h \approx 5$ cm is larger than at C-band, suggesting that L-band signals penetrate the shallow layer of wet snow and in-

teract with a rough interface of glacier ice ($\epsilon_r = 3.2$ [9]). Thawed lakes appear more clearly than at C-band.

The inversion results show that SAR could help map snow wetness in the Greenland soaked-snow zone, thereby providing valuable information for estimating surface fluxes and fresh water production over the ice sheet. C-band VV from ERS-1 could separate wet snow from dry snow, but the addition of at least one polarization (e.g. C-band HH from RADARSAT) could permit a more reliable mapping of snow wetness.

Percolation facies: Unusually strong radar reflectivities and large circular ($\mu_C = \sigma^o_{RR}/\sigma^o_{RL}$, where R and L mean right and left circular polarizations) and linear ($\mu_L = \sigma^o_{HV}/\sigma^o_{HH}$) polarization ratios are recorded at C- and L- band from the percolation facies. To the best of our knowledge, no other terrestrial surface shows similar radar properties, and the only other known objects with similar exotic radar properties are the icy Galilean satellites of Jupiter [10-11]. The radar signatures from the percolation zone show a different behavior at 68-cm wavelength (Fig. 4) and at small incidence angles, but this is not surprising since the subsurface structures responsible for the unusual radar echoes from Greenland and from the icy satellites probably are radically different. Nevertheless, the Greenland's percolation zone provides a uniquely accessible, natural laboratory for studying exotic radar processes in a geological context and for improving our understanding of radar scattering from distant icy objects.

Years ago, Zwally [12] suggested that the low emission properties of the percolation zone could be due to volume scattering from ice features buried in the firn and created by summer melt. Swift et al. [1] also noted unusual radar reflectivities from the percolation facies, and suggested that radars could estimate the density of these ice features. Recent surface-based radar observations at Crawford Point [13] at 5.4 and 2.2 cm further indicate that most of the scattering takes place in the most recent annual layer of buried ice bodies, and that surface scattering from the top 20 cm of the ice sheet dominates at small incidence angles. The exact scattering mechanism responsible for the unusual echoes is still unknown, and little information is available about the spatial distribution and geometric characteristics of ice lenses, layers, and pipes [5, 14-16]. Rayleigh scattering does not explain the radar properties of the percolation facies because the radar cross-sections do not decrease as λ^4, and even large snow grains cannot generate the σ^o_{HV} values recorded in the percolation zone. Similarly, natural rough surfaces of wavelength-size rms height ($h \geq 25$ cm) do not seem capable of generating radar signals similar to those recorded in the percolation zone.

Coherent backscatter is capable of interpreting the radar properties from the icy satellites [17] and is consistent with their geology and formation history [10]. Coherent backscatter occurs when electromagnetic waves traveling along time-reversed paths constructively interact in the backscattering direction, yielding enhanced radar reflectivities, and preserving the handedness of circular-polarized signals (as opposed to specular reflections). Coherent backscatter only requires a low-loss medium, i.e. long photon pathlengths. High radar reflectivities and circular polarization ratios greater than unity occur when the scatterers in the lossy medium are larger in size than the radar wavelength [18], and when the dielectric constrast is low [19]. Given typical sizes of ice layers and ice pipes [5, 14-16], and the relative transparency of dry, cold snow at microwave frequencies, coherent backscatter from massive ice inclusions created by summer melt events could explain the radar echoes from Greenland. Coherent backscatter however predicts [19] that μ_C should decrease with increasing θ, whereas AIRSAR shows the opposite trend. This discrepancy could be due to strong backreflection from wind crusts present in the top 20 cm of the ice sheet [13] which could yield small values of μ_C and μ_L at small incidence angles.

Since ice layers and ice pipes are anisotropic scatterers larger in size than the wavelength, we examined the high frequency solution of simple objects to determine whether unusual radar echoes can be predicted and better interpreted. We used dielectric cylinders because an exact analytical solution exists for computing their radar cross-sections [20]. In principle, highly depolarized signals could result from 180° phase shifts between HH and VV, i.e. internal reflections within the icy cylinders. Although ice layers and ice pipes are not cylinders, it is a first-order approximation that incorporates their dielectric properties, differences in size along perpendicular directions, and principal dimensions larger than the radar wavelength. From the numerical solution for one cylinder, we generated the response from a distribution of cylinders by applying a rotation matrix of uniform distribution in angle to the scattering matrix from one cylinder, and incoherently added the returns from different cylinders. When the dielectric contrast between the cylinders and the matrix is low, for a large number of a/λ values, we found that $\phi_{HHVV*} = 180°$, $\mu_L > 0.5$ and $\mu_C > 1$ (Fig. 5). By averaging the radar returns from a distribution of cylinders about 20-30 cm in size, we obtain $\mu_L > 0.37$, $\mu_C > 1.4$, and radar reflectivities close to 0 dB as observed for Greenland. The advantage of this modeling approach compared to the coherent backscatter theory is to provide a more readily understood interpretation of the radar echoes and a model that is easily invertible.

CONCLUSIONS

Monitoring the percolation facies using SAR could be of considerable importance. The Greenland percolation zone extends over a large range of latitudes and provides one of the most significant land bodies that could reveal climatic and hydrologic trends in the Arctic. The large contrast in radar backscatter between the percolation zone and the surrounding snow zones, and the fine spatial resolution of SARs should permit the fine monitoring of horizontal shifts in the boundaries of the percolation zone that probably no other instrument can detect. The percolation zone defines critical hydrological limits where melt-water re-freezes in place instead of being re-distributed in the ocean waters as in the soaked-snow and ablation zones. Measuring the volume of melt-water stored in the percolation zone each summer from SAR data is essential to improve current estimates of the mass balance of Greenland [16]. Our results are encouraging that multi-channel SAR instruments could estimate this ice-water volume. Furthermore, monitoring of the percolation facies with SAR could provide a more sensitive detection of spatial and temporal changes in the strength summer melting than that provided by monitoring changes in surface elevation measured by altimeters because melting in the dry snow zone will probably first increase the areal extent of the percolation zone [16].

ACKNOWLEDGEMENTS This work is supported by Dr. R. Thomas, Polar Research Program, NASA HQ, and was carried out at the Jet Propulsion Laboratory, California Institute of Technolgy, under contract with the National Aeronautics and Space Administration.

REFERENCES

[1] Swift, C. T., P. S. Hayes, and J. S. Herd, Airborne microwave measurements of the southern Greenland ice sheet, *J. Geophys. Res.* 90 B2, 1983-1994, 1985.

[2] Bindschadler R.A., K.C. Jezek, and J.P. Crawford, Glaciological investigations using the synthetic aperture radar imaging system, *Annals of Glaciology* **9**, 1-7, 1987.

[3] Vornberger, P.L., and R.A. Bindschadler, Multi-spectral analysis of ice sheets using co-registered SAR and TM imagery, *Int. J. Rem. Sens.* **13**, 637-645, 1992.

[4] Jezek, K., M.R. Drinkwater, J.P. Crawford, R. Bindschadler, and R. Kwok, Analysis of synthetic aperture radar data collected over the southwestern Greenland ice sheet, *J. of Glaciology* **39**, 131, 1993.

[5] Benson, C., Stratigraphic studies of the snow and firn of the Greenland ice sheet, *US Army Snow Ice and Permafrost Res. Estab.*, Res. Rep. 70, 1962.

[6] Alley, R. B., and B. R. Koci, Ice-core analysis at site A, Greenland: Preliminary results, *Annals of Glaciology* **10**, 1-4, 1988.

[7] van Zyl, J.J. and others, Measuring soil moisture with imaging radars, in preparation, 1993.

[8] Ulaby, F.T., Moore R.K., and Fung A.K., *Microwave Remote Sensing: Active and Passive*, Vol. III, Artech House, Norwood, Mass., 1986.

[9] Mätzler C., Applications of the interaction of microwaves with the natural snow cover, in *Remote Sensing Reviews*, F. Becker (Edt), Vol. 2, Issue 2, Harwood Academ. Pub., London, 391 pp., 1987.

[10] Ostro, S. J., and others, Europa, Ganymede, and Callisto: New radar results from Arecibo and Goldstone, *J. Geophys. Res.* **97** E 11, 18227-18244, 1992.

[11] Rignot, E., S. J. Ostro, J. J. van Zyl, and K. Jezek, Unusual radar echoes from the Greenland ice sheet, subm. *Science*, April 1993.

[12] Zwally, H. J., Microwave emissivity and accumulation rates of polar firn, *J. Glaciol.* **18**, 195-215, 1977.

[13] Jezek, K., and P. Gogineni, Microwave remote sensing of the Greenland ice sheet, *IEEE Geosc. and Rem. Sens. Soc. Newsletter*, Dec. 1992.

[14] Echelmeyer, K., W. D. Harrison, T. S. Clarke, and C. Benson, Surficial glaciology of Jakobshavns Isbrae, West Greenland: Part II. Ablation, accumulation and temperature, *J. of Glaciology* **38**, 169, 1992.

[15] Pfeffer, W. T., T. H. Illangasekare, and M. F. Meier, Analysis and modeling of melt-water refreezing in dry snow, *J. of Glaciology* **36**, 238-246, 1990.

[16] Pfeffer, W. T., M. F. Meier, and T. H. Illangasekare, Retention of Greenland runoff by refreezing: Implications for projected future sea level change, *J. Geophys. Res.* **96**, C12, 22,117-22,124, 1991.

[17] Hapke, B., Coherent backscatter and the radar characteristics of outer planet satellites, *Icarus* **88** 407-417, 1990.

[18] Peters, K. J., Coherent-backscatter effect: A vector formulation accounting for polarization and absorption effects and small or large scatterers, *Phys. Rev. B* **46**, 801-812, 1992.

[19] Mishchenko, M. I., Polarization characteristics of the coherent backscatter opposition effect, *Earth, Moon, and Planets* **58**, 127-144, 1992.

[20] Bohren, C. F., and D. R., Huffman, *Absorption and Scattering of Light by Small Particles*, Wiley, NY, 1983.

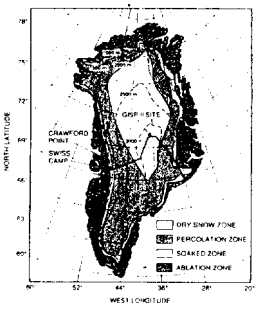

Figure 1. Map of Greenland showing the 4 snow zones defined by Benson (8), the flight track of AIRSAR (continuous thick line), ice sheet elevation contours (dashed line), and the location of the Swiss Camp, Crawford Point, and the GISP II site. Melting rarely occurs in the dry-snow zone; forms massive, buried, solid-ice inclusions in the percolation zone; saturates the snow with liquid water in the soaked snow-zone; and removes the seasonal snow cover and ablates the glacier ice in the ablation zone.

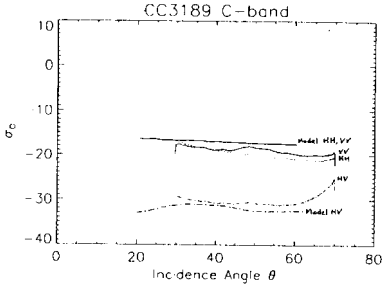

Figure 2. Radar backscatter σ^o measured by AIRSAR at C-band, at HH-, HV-, and VV- polarization vs θ in the dry snow zone near the GISP II site. Model predictions (dotted lines) for scattering from a half-space of dry snow using the radar backscatter model of J.C. Shi, UCSB. The snow temperature is -10°C, the ice fraction is 0.349 (snow density is 0.32 g/cm^3), the grain diameter is 0.2 ±0.05 mm [6] and the air-snow interface has a rms height of 0.78 cm and a correlation length of 13.8 cm.

Figure 3. C-band VV image of scene 3152 acquired by AIRSAR in the soaked-snow zone, west of the Swiss camp. AIRSAR is flying from right to left, looking to its left. Near-range is on top. The imaged region is 10 km by 10 km in size.

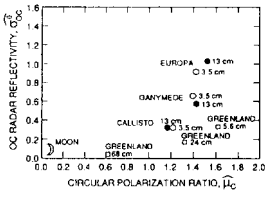

Figure 4. Points for extraterrestrial targets are averages of disk-integrated measurements at various subradar longitudes. Disc-resolved echo spectra, which are equivalent to brightness scans through a slit parallel to the projected spin vector, show hardly any variation in μ_C across the satellite discs. For Greenland, points are averages of measurements that span incidence angles, θ, from 18° to 66°.

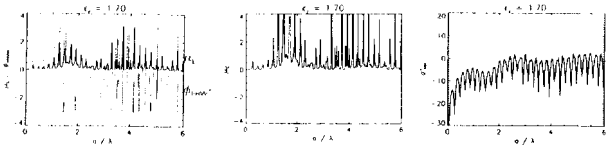

Figure 5. Model predictions of radar scattering from discrete, dielectric cylinders embedded in a lossy medium for different values of the relative diameter a/λ of the cylinders. The relative dielectric constant of the icy cylinders in dry snow is 1.7. The cylinders are assumed 1 m in length, with 5 cylinders per square meter. σ^o_{HH} is proportional to the square of the length of the cylinders, and to the density of cylinders; whereas μ_L and μ_C only depend on a/λ. The model results indicate that the ice-bodies are about 20-30 cm in diameter, 1 m in length, with a density of 5 cylinders per square meter.